

See discussions, stats, and author profiles for this publication at: <https://www.researchgate.net/publication/6951149>

Temperature Dependence of the Mass Accommodation Coefficients of 2-Nitrophenol, 2-Methylphenol, 3-Methylphenol, and 4-Methylphenol on Aqueous Surfaces

ARTICLE *in* THE JOURNAL OF PHYSICAL CHEMISTRY A · APRIL 2005

Impact Factor: 2.69 · DOI: 10.1021/jp0474430 · Source: PubMed

CITATIONS

9

READS

26

3 AUTHORS, INCLUDING:



Gontrand Leyssens

Université de Haute-Alsace

12 PUBLICATIONS 43 CITATIONS

SEE PROFILE



Florent Louis

Université des Sciences et Technologies de Li...

45 PUBLICATIONS 401 CITATIONS

SEE PROFILE

Temperature Dependence of the Mass Accommodation Coefficients of 2-Nitrophenol, 2-Methylphenol, 3-Methylphenol, and 4-Methylphenol on Aqueous Surfaces

Gontrand Leyssens, Florent Louis,* and Jean-Pierre Sawerysyn

Physico-Chimie des Processus de Combustion et de l'Atmosphère (PC2A), UMR CNRS 8522, FR CNRS 2416 Centre d'Etudes et de Recherche Lasers et Applications (CERLA), Université des Sciences et Technologies de Lille, 59655 Villeneuve d'Ascq Cedex, France

Received: June 14, 2004; In Final Form: January 7, 2005

The uptake of 2-nitrophenol, 2-methylphenol, 3-methylphenol, and 4-methylphenol on aqueous surfaces was investigated between 278 and 303 K, using the wetted-wall flow tube technique coupled with UV absorption spectroscopic detection. The uptake coefficients γ were found to be independent of the aqueous phase composition and of the gas–liquid contact times. In addition, the uptake coefficients and the derived mass accommodation coefficients α show a negative temperature dependence in the temperature range studied. The mass accommodation coefficients decrease from 5.2×10^{-3} to 8.3×10^{-4} , from 5.0×10^{-3} to 3.1×10^{-4} , from 6.7×10^{-3} to 7.3×10^{-4} , and from 1.2×10^{-2} to 5.9×10^{-4} for 2-nitrophenol, 2-methylphenol, 3-methylphenol, and 4-methylphenol, respectively. These results are used to discuss the incorporation of these species into the liquid using the nucleation theory. These data combined with the Henry's law constants were used to estimate the partitioning of the phenolic compounds between gaseous and aqueous phases and the corresponding atmospheric lifetimes under clear sky (τ_{gas}) and cloudy conditions ($\tau_{\text{multiphase}}$) have then been derived.

I. Introduction

Phenols and nitrophenols are known to be hazardous to health¹ and are among the most important classes of toxic anthropogenic organic compounds in the atmosphere.² Phenolic compounds occur naturally in various plants, in crude oil, and coal tar. Low levels of concentration are present in automobile exhaust, stack emissions from municipal waste incinerators, and emissions from the incineration of vegetable matter. Methylphenols (cresols) have a wide variety of uses as solvents or disinfectants or as intermediates in the production of numerous other substances. These compounds are most commonly used in the production of fragrances, antioxidants, dyes, pesticides, and resins. 2-Methylphenol (*ortho*-cresol) and 4-methylphenol (*para*-cresol) are used in the production of lubricating oils, motor fuels, and rubber polymers, whereas 3-methylphenol (*meta*-cresol) is used in the manufacture of explosives. 2-Nitrophenol is used mainly to make dyes, paint coloring, rubber chemicals, and substances that kill molds.

In the atmosphere, nitrophenols and methylphenols are originated by the gas phase reaction of benzene and toluene with the OH radical in the presence of NO_x or the nitrate radical.^{3–10} Phenolic compounds have been identified and quantified in atmospheric air in the ng m⁻³ range and in different condensed phases in the atmosphere (rain, snow, fog) from the level of $\mu\text{g L}^{-1}$ for alkyl phenols up to the range of mg L⁻¹ for nitrated phenols.^{1,11–23}

To better predict the fate, the transport, and the removal of these pollutants in the troposphere, the uptake kinetics of gas phase phenolic compounds by aqueous surfaces has to be investigated. Heterogeneous processes begin with precursor gas molecules colliding with the surface of liquid droplets in clouds, fog, and dew then crossing into the bulk. A key parameter that deter-

mines the transfer rate of trace gas into atmospheric droplets is the mass accommodation coefficient, α , which is the probability that a molecule striking a liquid surface enters the liquid phase. It determines the maximum flux of gas into a liquid. However, the mass accommodation coefficient does not describe the overall uptake kinetics because it does not take into account limitations introduced by diffusion processes (in both phases), by saturation phenomena of the interface or by chemical transformation in the liquid phase. To take such limitations into account, the overall uptake γ can be defined and considered as a sequence of resistances of the individual processes:²⁴

$$\frac{1}{\gamma} = \frac{1}{\gamma_{\text{diff}}} + \frac{1}{\alpha} + \frac{1}{\gamma_{\text{sat}} + \gamma_{\text{rxn}}} \quad (1)$$

where γ_{diff} , γ_{sat} , and γ_{rxn} correspond to the uptake coefficient according to gas phase diffusion, saturation and reactivity limitations, respectively. If experimental parameters are chosen so that one of these terms becomes rate limiting for the uptake, γ can be approximated by relatively simple analytic expressions for a cylindrical flow tube geometry:

diffusion limitation²⁵

$$\gamma_{\text{diff}} = \frac{3.66(2D_{\text{g}})}{\omega r} \quad (2)$$

saturation limitation²⁶

$$\gamma_{\text{sat}} = \frac{4HRT}{\omega} \sqrt{\frac{D_{\text{a}}}{\pi t}} \quad (3)$$

reactivity limitation²⁷

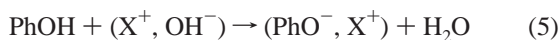
$$\gamma_{\text{rxn}} = \frac{4HRT}{\omega} \sqrt{D_{\text{a}} k_{\text{rxn}}} \quad (4)$$

where D_{g} and D_{a} are the gaseous and aqueous phase diffusion coefficients, ω is the mean molecular velocity of the trace gas,

* To whom correspondence should be addressed. E-mail: florent.louis@univ-lille1.fr. Fax: (33)-3-20436977.

r is the radius of the flow tube, H is Henry's law constant, R is the perfect gas constant, t is the gas/liquid contact time, and k_{rxn} is the pseudo first-order rate constant for a reaction in the liquid phase.

The reaction between aqueous solution of alkaline hydroxide (XOH) with a dissolved phenolic compound (PhOH)



has been routinely used in the laboratory to determine the concentration of the phenolic compounds in the gas phase.²⁸ The use of this liquid phase scavenger of phenols enabled a direct estimation of the mass accommodation coefficient ensuring that the total liquid phase resistance is negligible in comparison to the interfacial resistance due to gas phase diffusion and mass accommodation for the gas/liquid contact time scale used under our experimental conditions (see section III for detailed discussion). Equation 1 then is simplified to

$$\frac{1}{\gamma} = \frac{1}{\gamma_{\text{diff}}} + \frac{1}{\alpha} \quad (6)$$

and the uptake coefficient reflects the mass accommodation coefficient adjusted for the rate of gas transported to the surface.

This paper is devoted to the uptake kinetics of a series of four phenolic compounds onto aqueous surfaces over a temperature range of tropospheric interest. The experiments were performed using the wetted-wall flow tube technique coupled to a wavelength-resolved UV spectrometer. The values of mass accommodation coefficients obtained in this study are critically compared with the previously reported values for 2-nitrophenol and 3-methylphenol by Müller and Heal.²⁹ To the best of our knowledge, it is the first time that the mass accommodation coefficients have been determined for the 2-methylphenol and 4-methylphenol. Reactivity trends and implications in tropospheric multiphase chemistry are also discussed.

This article is organized as follows. Section I (current) presents an introduction. Experimental methods are reported in section II, and the results are presented and discussed in section III.

II. Experimental Methods

Uptake coefficients were measured using a wetted-wall flow tube combined with a UV spectrometer. A similar technique has been used to study the transport of gases into liquid for many years.^{25,27,29–37} The flow tube (Figure 1) consists of a vertically mounted Pyrex glass tube (90 cm long, and with an internal diameter of 1.4 cm) with a thermostated jacket to control the temperature of the aqueous film flowing slowly down the inner walls of the reactor. From a pressurized storage tank, the aqueous solutions are transported into a reservoir at the top of the flow tube where the upper 7 cm section is separated from the reaction zone by a glass cone internally recovered by a Teflon joint sleeve. To obtain a uniformly covered glass surface for each experiment, cleaning of the tube with a mixture of deionized water, and potassium hydroxide followed by thorough rinsing with deionized water was necessary. The aqueous solutions were collected at the bottom of the flow tube into a 6 L flask, which was refrigerated to a temperature below the one used in uptake experiments to prevent back-streaming of the water vapor up to the flow tube. Different contact times between trace gas and liquid surface were attained by changing injector position.

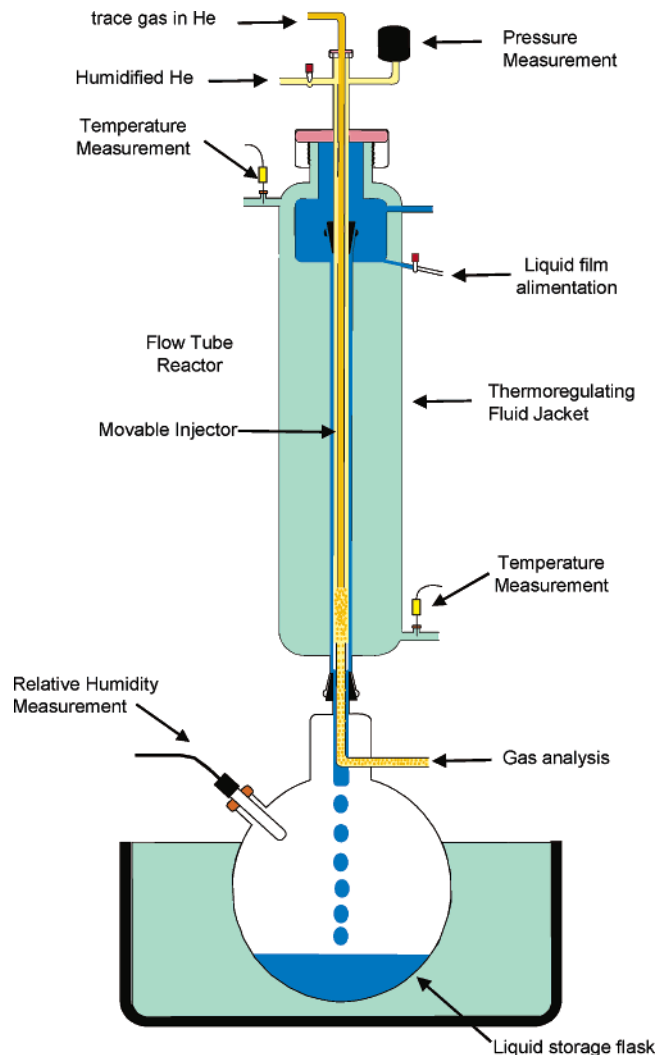


Figure 1. Schematic diagram of the wetted-wall flow tube.

Over the temperature range of tropospheric interest, phenolic compounds are in their condensed physical state. Nonhumidified carrier gas passed through a thermostated trap filled with the phenolic compound providing a continuous and constant concentration during the time of experiment.

The flow rates of the liquid film were in the range (0.3–0.5) $\text{cm}^3 \text{s}^{-1}$. The thickness and the flow velocity of the liquid film were estimated using the equations reported by Danckwerts.²⁷ At 293 K, for a typical flow rate of 0.4 $\text{cm}^3 \text{s}^{-1}$, the film was about 140 μm thick and its maximum velocity, v_{max} , at the surface, was estimated to be about 10 cm s^{-1} . Uncertainties in the calculation of the water thickness have been estimated to be about 10%. The Reynolds number of the liquid film was calculated as described by Utter et al.³⁰ to be about 10. Therefore, the film was expected to be in laminar flow under our experimental conditions ($Re < 250$ –400). Ripples in the film's surface were apparent for higher liquid flow rates ($> 1.0 \text{ cm}^3 \text{s}^{-1}$) leading to enhanced mass transport into the liquid.^{25,30} Visual inspection confirmed the absence of rippling in our experiments.

Regulated flow rates of trace gases were introduced in the reactor via a movable injector of 6 mm outer diameter. The main flow of He was passed through a thermostated water bubbler to avoid evaporative cooling or drying of the liquid film and introduced at the top of the reactor. No water was added to the He flux transporting the trace gases through the injector and the ratio of He (injector)/He (main) was kept as low as

TABLE 1: Typical Experimental Conditions for the Uptake Kinetics of Phenolic Compounds by Water Surfaces

compound	<i>T</i> (K)	pH	pHe (Torr)	pH ₂ O (Torr)	<i>D_g</i> (cm ² /s)
2-nitrophenol	283–298	8.1–13.7	142–156	4–14	1.08–1.22
2-methylphenol	278–298	11.9–14.0	125–150	3.5–18.5	1.10–1.27
3-methylphenol	283–298	11.9–14.0	140–172	3.5–18.5	0.99–1.19
4-methylphenol	283–303	11.5–13.9	154–170	4–25	0.97–1.11

possible in all experiments, with a maximum of 15% of nonhumidified carrier gas entering through the injector. Hanson et al.²⁵ showed that the He carrier gas entering the top of the flow tube was uniformly saturated with water vapor within approximately 10 cm. The upper 15 cm of the aqueous film was not used for uptake measurements to allow thorough mixing and equilibration of water vapor and main pre-humidified He flow. Under these conditions, the total gas flow velocity can be estimated by the following equation:²⁵

$$c = \frac{760FT}{273\pi r^2(P - p_{\text{H}_2\text{O}})} \quad (7)$$

where *F* is the sum of the measured flow rates for all dry gases (cm³ s^{−1}), *T* and *r* are respectively the temperature (K) and the radius (cm) of the flow tube, *P* is the total pressure in the flow tube (Torr), and *p*_{H₂O} is the vapor pressure of water (Torr) at *T*. The partial pressure of the water vapor was determined from the humidity measurements and the partial pressure of the phenolic compounds were considered negligible. The Reynolds number for a mixture of helium and water was calculated according to Utter et al.³⁰ Depending on gas flow velocity, it varied from 5 to 20, so that a laminar gas flow can be assumed. Uncertainties in the calculation of the gas flow velocity have been estimated to be about 5%.

The gases left the flow tube through a sidearm below the wetted-wall flow tube and into a 100 cm length absorption cell. Changes in the trace gases concentration were measured by wavelength-resolved UV spectroscopy at the wavelength of maximum absorption cross section typically in the region of 270–280 nm. The output of a deuterium lamp (Hamamatsu L7295) was collimated through an absorption cell (100 cm long Pyrex cell equipped with quartz windows) and focused into the entrance slit of a *f*/3.5 aperture monochromator equipped with a 1200 groove/mm grating (Jobin Yvon H10), which dispersed the light onto a photomultiplier detector (Hamamatsu R212). The monochromator is provided with a computer controlled wavelength stepping motor drive and a computerized data acquisition system consisting of analogue to digital circuitry. The initial concentrations of the phenolic compounds used in this work were in the range (2–7) × 10¹⁴ cm^{−3} corresponding to a level of concentration of 60–110 mg m^{−3}. Typical experimental conditions are reported in Table 1.

Chemicals. Pure 2-nitrophenol (C₆H₅NO₃, GC grade, ≥98%), 2-methylphenol (C₇H₈O, GC grade, ≥99.5%), 3-methylphenol (C₇H₈O, GC grade, ≥99%), and 4-methylphenol (C₇H₈O, GC grade, ≥98%) were obtained from Fluka Chemical Company and used without further purification. Helium (BTG-GTB, >99.996%) was purified by circulating through molecular sieves with indicator. Solutions of KOH (Riedel de Haën, >85%) used as the scavenger of phenolic compounds varied in concentrations from 10^{−6} to 1 M. The solutions were prepared using deionized water (resistivity 18 MΩ cm) and reagent-grade pellets.

Measurement Procedure. The trace gas loss rate in the flow tube was measured as a function of the position of the movable injector, i.e., as a function of gas/liquid contact time *t*. The length *l* of interaction zone could be varied up to 55 cm. The measured

rate constant *k_w* was always first-order with respect to the gas phase concentration of the phenolic compound (PhOH):

$$[\text{PhOH}]_{z_2} = [\text{PhOH}]_{z_1} \exp\left(-k_w \frac{\Delta z}{c}\right) \quad (8)$$

where [PhOH]_{*z*1,2} are the PhOH concentrations at injector positions *z*₁ and *z*₂ and Δ*z* represents the distance between the two positions. The ratio Δ*z*/*c* defines the gas residence time more often named gas/liquid contact time.

In our operating conditions, the plug flow approximation has been assumed taking into account the fact that the relative velocity of gas flow and liquid film leads to estimated uncertainties of 10–20% in *k_w* and then in *γ* values. By taking into account the geometric liquid surface exposed to the gas phase and the volume of the flow tube, one can extract, from eq 8 after time integration, an expression for the uptake coefficient *γ*:³⁸

$$\gamma = \frac{2rk_w}{\omega} \quad (9)$$

As an example, Figure 2 shows the variation of the ln ([2-nitrophenol]/[2-nitrophenol]₀) as a function of the contact time *t* corresponding to the uptake kinetics of 2-nitrophenol onto aqueous films of [KOH] = 0.01 M at different temperatures. The slopes yield *k_w* and thus define *γ* according to eq 9 for each experiment. The mass accommodation coefficients corresponding to each rate constant *k_w* are obtained by the use of eq 6. Depending on the temperature and on the phenolic compound, the mass accommodation coefficients reported in this paper correspond to the average of a series of 7 to 16 replicates during which the rate constants *k_w* were obtained by moving the injector from 4 to 8 different positions. Estimated uncertainties correspond to the 95% confidence limit intervals using the student's *t*-distribution.³⁹

At a total gas flow velocity *c* of 40 cm s^{−1} and at high uptake rates, the correction due to radial diffusion estimated using eq 2 can be significant on the uptake values (from 5% to a factor

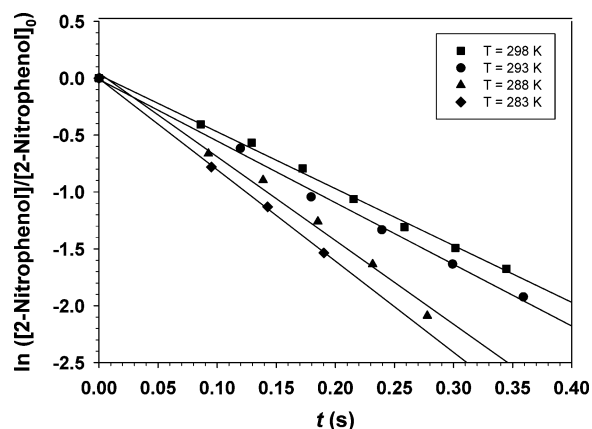


Figure 2. Evolution of ln([2-nitrophenol]/[2-nitrophenol]₀) as a function of the contact time *t* at different temperatures corresponding to the uptake kinetics of 2-nitrophenol onto aqueous films of [KOH] = 0.01M.

TABLE 2: Pressure-Independent Diffusion Coefficients (Torr cm² s⁻¹) of Phenolic Compounds in Water and Helium Using the Method of Fuller et al.⁴³

<i>T</i> (K)	2-nitrophenol		2-methylphenol		3-methylphenol		4-methylphenol	
	<i>D_g</i> (X/H ₂ O)	<i>D_g</i> (X/He)	<i>D_g</i> (X/H ₂ O)	<i>D_g</i> (X/He)	<i>D_g</i> (X/H ₂ O)	<i>D_g</i> (X/He)	<i>D_g</i> (X/H ₂ O)	<i>D_g</i> (X/He)
278			69.4	184.9				
283	72.1	195.3	71.6	190.7	71.6	190.7	71.6	190.7
288	74.4	201.4	73.8	196.7	73.8	196.7	73.8	196.7
293	76.6	207.5	76.1	202.7	76.1	202.7	76.1	202.7
298	78.9	213.8	78.3	208.8	78.3	208.8	78.3	208.8
303							80.7	215.0

of 2). Equation 2 has been used to correct the measured uptake from the effect of the gas phase diffusion. The geometry-dependent factor of 3.66 in eq 2 is valid when axial diffusion can be neglected; i.e., if the flow velocity is much greater than the axial diffusion velocity. This condition is true when the Peclet number⁴⁰ ($2rc/D_g$) is greater than 10. Peclet numbers between 40 and 80 were typical of the experimental conditions used in our work.

The value of the overall gas phase diffusion coefficient D_g (in cm² s⁻¹) was calculated for each experiment from the following equation:

$$\frac{1}{D_g} = \frac{p_{\text{H}_2\text{O}}}{D_g(\text{X/H}_2\text{O})} + \frac{p_{\text{He}}}{D_g(\text{X/He})} \quad (10)$$

where $p_{\text{H}_2\text{O}}$ and p_{He} are the partial pressures of water and helium in each gaseous mixture experimentally investigated, $D_g(\text{X/H}_2\text{O})$ and $D_g(\text{X/He})$ the diffusion coefficients for the binary gas-systems (X/H₂O and X/He), respectively. As the binary diffusion coefficients for all species X studied here were not experimentally known, they should be calculated from theoretical methods⁴¹ or methods using empirical correlations.^{42,43} Table 1S of the Supporting Information gathers all molecular parameters necessary for these calculations. Due to the good agreement obtained between the calculated and experimental values of diffusion coefficients for a great number of binary gas systems, the methods proposed by Fuller et al.⁴³ have been largely used in the literature even for gas systems including polar components.^{29,44,45} Table 2 gives the values of the pressure-independent binary diffusion coefficients $D_g(\text{X/H}_2\text{O})$ and $D_g(\text{X/He})$ obtained for all species studied here from Fuller's methods. However, as shown in Table 1S, all phenolic species of interest are characterized by a dipole moment, suggesting a better choice in the use of methods taking into account the dipole–dipole interactions. To evaluate the effects of dipole–dipole interactions on the estimates of diffusion coefficients under our experimental conditions, we have applied to the most polar species investigated in this work (2-nitrophenol, $\mu = 6.35$ D⁴⁶) a method suggested by Brokaw⁴⁷ and presented by Reid et al.⁴¹ for binary mixtures containing polar components. The calculated values of the binary pressure-independent gas diffusion coefficients are reported in the Tables 2S of the Supporting Information. For 2-nitrophenol at 298 K, $D_g(\text{X/H}_2\text{O})$ and $D_g(\text{X/He})$ are respectively about –40% and +7% different from the values given by the Fuller treatment. The mass accommodation coefficients calculated for all compounds using this treatment are reported in the Table 3S of the Supporting Information. When applied to our experimental conditions in the case of the 2-nitrophenol, the values of the mass accommodation coefficients using the Brokaw method⁴⁷ for the estimation of the diffusion coefficients were different only by 5% to 20% compared to the values obtained by the application of the Fuller et al. method,⁴³ which does not consider the dipole–dipole interactions. In the case of the cresol isomers

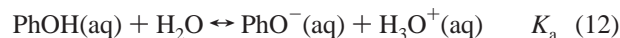
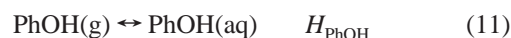
that exhibit dipole moments (about 1.5 D) much less than 2-nitrophenol, and at the two lower studied temperatures (278 and 283 K), the use of the Brokaw method⁴⁷ leads systematically to decrease the mass accommodation coefficients by a factor of about 1.4 to 2.6. At these temperatures, polar interactions of phenolic compounds with water are expected to be less important. The differences observed in the calculated values of the mass accommodation are due to the interactions of phenolic compounds with helium under our operating conditions. For binary systems including only few polar components (alcohols) and aromatic species (benzene, bromobenzene), the Fuller et al. procedure yielded the smallest average error of 5.4%.⁴³ However, even if the values of the mass accommodation coefficients obtained using Fuller's method are in relatively good agreement with the ones calculated using the Brokaw method, this does not imply that Fuller's method including polar components is not entirely correct. For only comparison purposes with previously reported paper for phenolic compounds,²⁹ we have chosen Fuller's method for estimation of binary gas diffusion coefficients.

III. Results and Discussion

III.1. Determination of the Rate-Limiting Step for the Uptake. As shown in eq 1, the overall uptake γ can be considered as a sequence of resistances of the individual processes. To determine the rate-limiting step for the uptake of the gas phase phenolic compounds, experiments were performed by varying the composition of the aqueous phase and the gas/liquid contact time. All uptake experiments used for the determination of the mass accommodation coefficients were performed for pH values of the bulk solution greater than the pK_a value of the phenolic compound.

In this section, the results obtained for 2-nitrophenol are presented as an example. Similar results have been obtained for the three isomers of cresol.

The chemical equilibria describing the solubility of the gaseous phenolic compound (PhOH) are as follows:



As pointed out by Schwartz and Freiberg,⁴⁸ the solubility of PhOH can be expressed as an effective Henry's law constant given by

$$H^*_{\text{PhOH}} = H_{\text{PhOH}} \left(1 + \frac{K_a}{[\text{H}_3\text{O}^+]} \right) \quad (13)$$

where $H = 90 \text{ M atm}^{-1}$ ⁴⁹ is the physical Henry's law constant for 2-nitrophenol at 293 K. If an equilibrium state at the interface between the gaseous 2-nitrophenol and its aqueous counterpart is assumed, it becomes possible to calculate the value of the

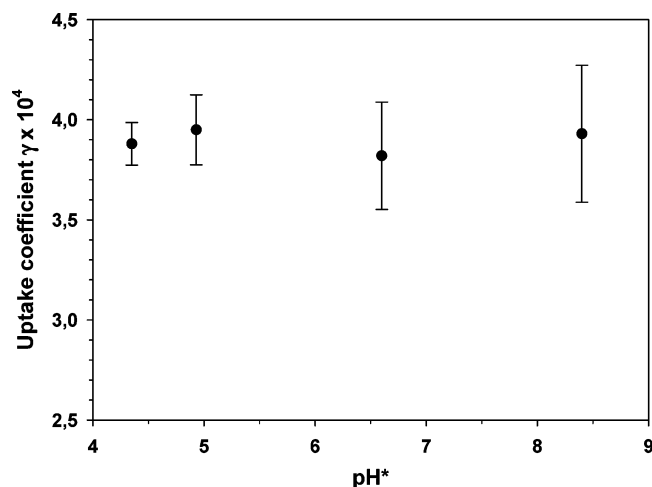


Figure 3. Uptake coefficient for 2-nitrophenol as a function of pH* at 293 K.

pH at the liquid film's surface (pH*) by solving the equilibria equations to give

$$[\text{H}_3\text{O}^+] = H' \pm (H'^2 + K_w + K_a[\text{PhOH}])^{1/2} \quad (14)$$

where

$$H' = ([\text{H}_3\text{O}^+]_0 - K_w/([\text{H}_3\text{O}^+]_0)/2 \quad (15)$$

where $[\text{H}_3\text{O}^+]_0$ is the initial concentration of the hydronium ion (bulk concentration) and K_w is the equilibrium constant for water.

According to eqs 14 and 15, calculated values for pH* and the ones of the effective Henry's law constant are given in Table 3. It is worth noticing that the solubility of 2-nitrophenol increases only significantly for pH* higher than the $\text{p}K_a$ value ($\text{p}K_a = 7.2^{39}$) suggesting that the observed values of γ for 2-nitrophenol should be higher when the surface's pH is increased. Figure 3 depicts the evolution of the measured γ uptake coefficient as a function of the surface liquid film pH* at 293 K for 2-nitrophenol. In the contrast of the expected evolution of γ as a function of pH*, any significant dependence of the uptake coefficient was not observed under our operating conditions within estimated statistical uncertainties (95% confidence limit interval). However, the solubility effects can be evaluated using the characteristic time τ_p necessary for the surface to be saturated, as demonstrated by Schwartz and Freiberg:⁴⁸

$$\tau_p = (4RTH/\omega\alpha)^2 D_a \quad (16)$$

In the case of the 2-nitrophenol at 293 K ($\alpha = 8.3 \times 10^{-4}$, $H = 90 \text{ M atm}^{-1}$,⁴⁹ $\omega = 21296 \text{ cm s}^{-1}$, $D_a = 8.1 \times 10^{-6} \text{ cm}^2 \text{ s}^{-1}$), the calculated value for τ_p is about 2 s so that the solubility effects should not be seen in our operating conditions. Furthermore, the exposure time of the liquid film to the gas is much lower than τ_p .

Otherwise, the thickness of the water film accessible during the exposure time can be evaluated from the expression $(D_a t)^{0.5}$ ⁵⁰ to be about 17 μm , which is largely smaller than the thickness of the liquid film (140 μm).

Based on these observations and due to the fact that the measured uptake coefficient is independent of the bulk concentration in the studied pH range, it was possible to conclude that the limitation due to aqueous phase reaction was not rate-

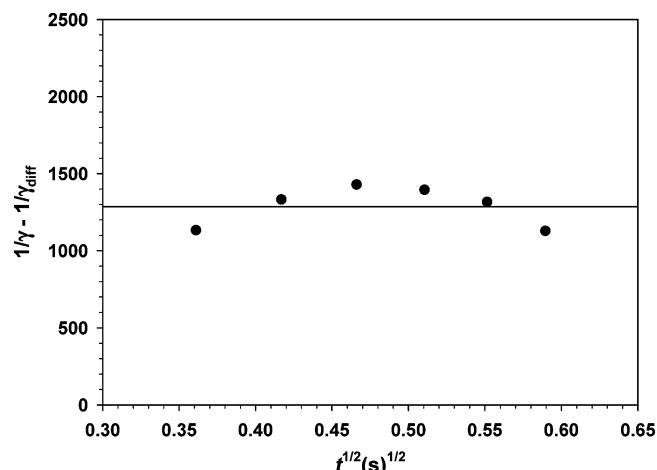


Figure 4. $1/\gamma - 1/\gamma_{\text{diff}}$ plotted as a function of $t^{1/2}$ for 2-nitrophenol for the uptake of 2-nitrophenol onto aqueous films of $[\text{KOH}] = 0.01 \text{ M}$ at 298 K.

TABLE 3: Effective Henry's Law Constant H^* for 2-Nitrophenol at 293 K for Different pH Values at the Surface of the Liquid Film

pH (bulk solution)	pH* (surface)	H^* (M atm^{-1})
8.1	4.4	90
10.2	4.9	91
11.9	6.6	112
13.7	8.4	1502

limiting then γ_{rxn} , defined by eq 4, could be neglected and eq 1 is simplified as follows:

$$\frac{1}{\gamma} = \frac{1}{\gamma_{\text{diff}}} + \frac{1}{\alpha} + \frac{1}{\gamma_{\text{sat}}} \quad (17)$$

If γ_{sat} is replaced by its expression taken from eq 3, we obtained

$$\frac{1}{\gamma} = \frac{1}{\gamma_{\text{diff}}} + \frac{1}{\alpha} + \frac{\omega\sqrt{\pi t}}{8HRT\sqrt{D_a}} \quad (18)$$

As shown in Figure 4, no dependence of $1/\gamma - 1/\gamma_{\text{diff}}$ as a function of the square root of the gas/liquid contact time t was observed for the uptake of 2-nitrophenol onto aqueous films of $[\text{KOH}] = 0.01 \text{ M}$ at 298 K. Same results were obtained by varying the temperature and the composition of the liquid film.

It is possible to conclude that the saturation of the aqueous phase was not rate-limiting step for the uptake of phenolic compounds by aqueous surfaces, thus γ_{sat} , defined by eq 3, could be neglected. Consequently, under our experimental conditions, the mass accommodation coefficient is equal to the overall uptake corrected for limitations due to gas phase diffusions as expressed in eq 6.

III.2. Mass Accommodation Coefficients. Table 4 gathers the mass accommodation coefficients α determined for the studied phenolic compounds at different temperatures. It can be noticed that the mass accommodation coefficients for all species studied show a negative temperature dependence. This behavior seems to be a general feature of mass accommodation for water-soluble species. Within the isomers of cresol, the magnitudes of α are ranked as 2-methylphenol < 3-methylphenol < 4-methylphenol and are consistent with the solubility of these compounds in water. For instance, $\alpha(293 \text{ K})$ of 4-methylphenol is approximately 4 times higher than that obtained for 2-methylphenol showing that the position of the $-\text{CH}_3$ group on the aromatic ring largely influences the uptake process.

TABLE 4: Mass Accommodation Coefficients of the Studied Phenolic Compounds over the Temperature Range of Interest^a

T (K)	2-nitrophenol	2-methylphenol	3-methylphenol	4-methylphenol
278		$(5.0 \pm 0.4) \times 10^{-3}$		
283	$(1.2 \pm 0.6) \times 10^{-2}$ $(5.2 \pm 0.6) \times 10^{-3}$ $(8.2 \pm 2.5) \times 10^{-3}$	$(3.2 \pm 0.5) \times 10^{-3}$	$(1.2 \pm 0.3) \times 10^{-2}$ $(6.7 \pm 1.6) \times 10^{-3}$	$(1.2 \pm 0.2) \times 10^{-2}$
288	$(3.3 \pm 0.4) \times 10^{-3}$ $(5.9 \pm 1.8) \times 10^{-3}$	$(1.2 \pm 0.1) \times 10^{-3}$	$(3.7 \pm 0.4) \times 10^{-3}$ $(6.9 \pm 2.1) \times 10^{-3}$	$(5.7 \pm 0.6) \times 10^{-3}$
293	$(1.2 \pm 0.3) \times 10^{-3}$ $(1.5 \pm 0.5) \times 10^{-3}$	$(6.6 \pm 0.4) \times 10^{-4}$	$(1.6 \pm 0.5) \times 10^{-3}$ $(6.0 \pm 1.8) \times 10^{-3}$	$(2.7 \pm 0.3) \times 10^{-3}$
298				
303	$(8.3 \pm 0.3) \times 10^{-4}$	$(3.1 \pm 0.4) \times 10^{-4}$	$(7.3 \pm 0.8) \times 10^{-4}$	$(1.2 \pm 0.2) \times 10^{-3}$ $(5.9 \pm 0.5) \times 10^{-4}$

^a The given errors are calculated with a 95% confidence interval limit using the student's *t*-distribution. ^b Values in italics are taken from Müller and Heal²⁹ where errors have been estimated to 30%.

Values of the mass accommodation coefficients for 2-nitrophenol and 3-methylphenol have been previously measured by Müller and Heal²⁹ and they are listed in Table 3 for comparison purposes. Müller and Heal²⁹ have employed a wetted-wall flow tube combined to UV absorption detection and molecular bromine as the scavenger for the phenolic compounds. In the case of 2-nitrophenol, their values of α closely agree with ours especially if we take into account the quoted uncertainties. It can be noticed that the values reported by Müller and Heal²⁹ for the 3-methylphenol do not agree with our measurements at the two common studied temperatures. Their values are respectively 3.8 and 1.9 higher than ours at 293 and 288 K. Moreover the temperature dependence of the mass accommodation clearly does not exhibit the same behavior as the one obtained for all isomers of cresols, which seems to be largely more consistent with the observed reactivity patterns.

It has been shown by Jayne et al. that the mass accommodation coefficient could be expressed as²⁶

$$\frac{\alpha}{1-\alpha} = \exp\left(-\frac{\Delta G_{\text{obs}}^{\ddagger}}{RT}\right) \quad (19)$$

The parameter $\Delta G_{\text{obs}}^{\ddagger}$ can be regarded as the Gibbs free energy barrier of the transition state⁵¹ between the gaseous and solvated states ($\Delta G_{\text{obs}}^{\ddagger} = \Delta H_{\text{obs}} - T\Delta S_{\text{obs}}$). The values of ΔH_{obs} and ΔS_{obs} can be obtained from the experimental results by plotting the $\ln[\alpha/(1-\alpha)]$ as a function of $1/T$ as displayed in Figure 5 for the studied phenolic compounds. The slope of such a plot is equal to $-\Delta H_{\text{obs}}/R$ and the intercept is $\Delta S_{\text{obs}}/R$. However, the temperature range is considered too much limited to enable us to assess ΔS_{obs} with a good precision. The magnitudes of ΔH_{obs} and ΔS_{obs} are inversely proportional to the hydrogen

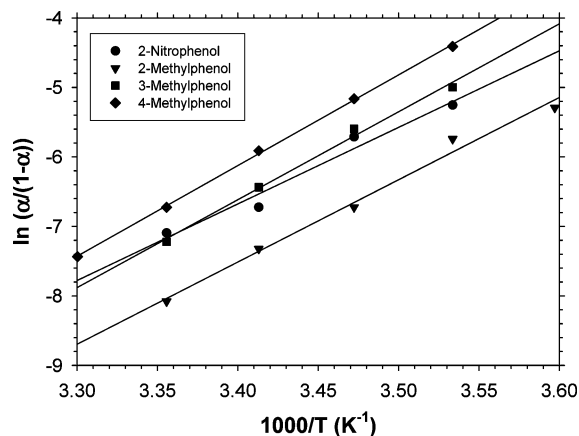


Figure 5. Evolution of $\ln(\alpha/(1-\alpha))$ as a function of $1/T$ for 2-nitrophenol, 2-methylphenol, 3-methylphenol, and 4-methylphenol.

TABLE 5: Measured Values of ΔH_{obs} and ΔS_{obs} ^a

molecule	ΔH_{obs} (kJ mol ⁻¹)	ΔS_{obs} (J mol ⁻¹ K ⁻¹)
2-nitrophenol	-91.6 ± 25.5	-345.0 ± 92.8
2-methylphenol	-98.4 ± 12.1	-397.1 ± 41.9
3-methylphenol	-105.2 ± 13.0	-412.6 ± 44.8
4-methylphenol	-108.5 ± 3.2	-419.8 ± 10.9

^a The given errors are calculated with a 95% confidence interval limit using the student's *t*-distribution.

bonding ability of the species. The more hydrophilic the species the smaller are the magnitudes of the values for both ΔH_{obs} and ΔS_{obs} . Their values for all the studied species are listed in Table 5. The magnitudes of ΔH_{obs} and ΔS_{obs} for the phenolic compounds are ranked as 2-nitrophenol < 2-methylphenol < 3-methylphenol < 4-methylphenol.

To explain the negative temperature dependence of the mass accommodation coefficient, Davidovits et al.²⁴ have developed a model, later modified by Nathanson et al.⁵² for the description of the dynamics. The penetration into the liquid was described as a continuous nucleation process at the interface where only clusters reaching a critical size N^* were taken up by the liquid phase. A molecule can enter water much more easily than its ability to act as a center of nucleation will be higher. Indeed the result of the observations, as reported for other water soluble compounds, is that an entropic barrier both controls gas/liquid accommodation kinetics and separates the surface state from the liquid. The nucleation theory accounts for the barrier in terms of critical cluster binding energy and surface tension. It was a simplified approach using bulk liquid phase properties based on the assumption of isotropic diffusion within the surface.

In this model, the parameter N^* was defined as the number of molecules in the cluster or the number of hydrogen bonds used to form the cluster by condensation. The value of N^* depends on the structure and the functionality of the specific molecule undergoing the uptake process. In this theory, Davidovits et al.²⁴ and Nathanson et al.⁵² demonstrated a direct relationship between ΔH_{obs} and ΔS_{obs} , governed by N^* . The changes of entropy ΔS_{obs} and enthalpy ΔH_{obs} can be determined from N^* by using the following equations reported by Nathanson et al.⁵²

$$\Delta H_{\text{obs}} = (-10(N^* - 1) + 7.53(N^{*2/3} - 1) - 0.1 \times 10) \times 4.184 \text{ (kJ mol}^{-1}\text{)} \quad (20)$$

$$\Delta S_{\text{obs}} = (-13(N^* - 1) - 19(N^* - 1) + 9.21(N^{*2/3} - 1) - 0.1 \times 13) \times 4.184 \text{ (J mol}^{-1}\text{ K}^{-1}\text{)} \quad (21)$$

Using these two equations, the calculated N^* values are 4.2, 4.4, 4.5, and 4.6 for 2-nitrophenol, 2-methylphenol, 3-meth-

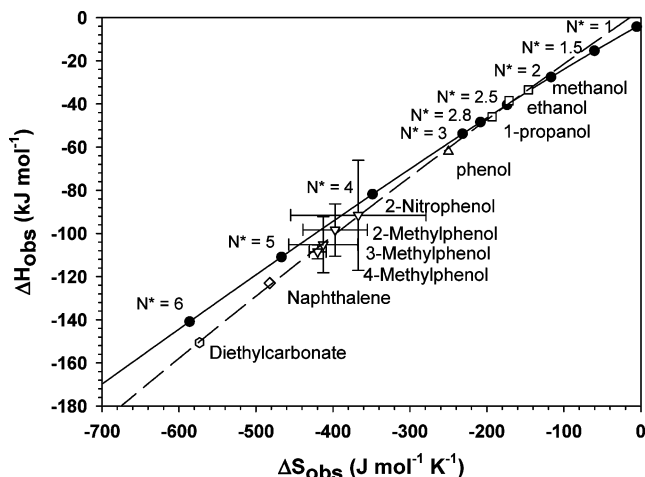


Figure 6. Plot of ΔH_{obs} versus ΔS_{obs} . The data (black circles and solid line) correspond to the use of eqs 20 and 21 as reported in ref 52. Data reported for aliphatic alcohols (methanol, ethanol, and 1-propanol), phenol, naphthalene, and diethylcarbonate are taken respectively from refs 51, 29, 52, and 45. The dashed line corresponds respectively to a second-order polynomial fit to the represented data. Our experimental results are represented with error bars given at the 95% confidence interval limit using the student's *t*-distribution.

ylphenol, and 4-methylphenol, respectively. These noninteger values represent an average number of molecules in a critical cluster at the interface. Because the chemical structures of the studied species are very similar, only small differences are observed for the N^* values.

Our results (ΔH_{obs} , ΔS_{obs}) are in very good agreement with the theoretical values calculated using eqs 20 and 21 and the experimental results given, for example, by Jayne et al. for aliphatic alcohols,²⁶ by Müller and Heal for phenol,²⁹ by Raja and Valsaraj for naphthalene,⁵³ or by Katrib et al. for diethyl carbonate,⁴⁵ as shown in Figure 6 where the black points correspond to the theoretical values calculated using eqs 20 and 21 for a data set containing 22 molecules.⁵²

For values of the critical cluster N^* larger than 3, a better fit to the experimental data (ΔH_{obs} and ΔS_{obs}) could be obtained using a second-order polynomial function (dashed line in Figure 6). Unfortunately, the data set used to obtain numerical values in eqs 20 and 21 contained only molecules for which the values of the critical size N^* are between 1.5 and 3.0.⁵² When N^* is greater than 3, it seems to be a general trend that a better fit to the experimental points (ours and those reported in refs 45 and 53) is obtained with the second-order polynomial function. However, experimental uncertainties reported for ΔH_{obs} and ΔS_{obs} are important and great care must be taken about the assumption that the model of nucleation will not work for large cluster sizes.

It is also worth noticing that the size of the critical cluster depends on the nature of a molecule containing an alcohol functional group. For a series of aliphatic alcohols, the value of N^* was estimated to be between 2 and 3²⁶ whereas the value of N^* obtained for phenol was about 3.2.²⁹ From the point of view of the uptake model, this implies that a critical cluster is more easily formed for aliphatic alcohols than around the aromatic species or that the phenyl ring decreases the effectiveness of the molecule as a nucleating agent.

III.3. Implications for Atmospheric Chemistry. The atmospheric implications of this work can be obtained from the comparison of the lifetimes (τ) of the phenolic compounds in the troposphere with respect to their removal by OH radicals in both the gas phase⁵⁴ and the aqueous phase.⁵⁵ To evaluate

the impact of a cloud on the atmospheric chemistry of phenolic compounds, we compare in this section their atmospheric lifetimes under clear sky (τ_{gas}), and cloudy conditions ($\tau_{multiphase}$).

The lifetime of A in the gas phase ($\tau_{A,gas}$) taking only into account the reaction of A with OH radicals, is defined as follows:

$$\tau_{A,gas} = \frac{[A]_g}{-d[A]_g/dt} = \frac{1}{k_{OH,g}[OH]_g} \quad (22)$$

where $k_{OH,g}$ is the rate constant of the gas phase reaction of OH radicals with A, $[OH]_g$ is the mean concentration of OH radicals, and $[A]_g$ is the concentration of A in the troposphere.

If we consider now the cloudy atmosphere as a multiphase reactor where both the gaseous and aqueous phases coexist, then the multiphase lifetime of A can be defined as⁵⁶

$$\tau_{A,multiphase} = \frac{[A]_g + [A]_{aq}}{-d[A]_g/dt - d[A]_{aq}/dt} \quad (23)$$

where $[A]_{aq}$ is the concentrations of A in the aqueous phase. At equilibrium, the fractions of A in the gas ($f_{A,g}$) and aqueous phases ($f_{A,aq}$) are the following ones:

$$f_{A,g} = \frac{[A]_g}{[A]_g + [A]_{aq}} = \frac{1}{1 + HRL_{wc}T} \quad (24)$$

$$f_{A,aq} = \frac{[A]_{aq}}{[A]_g + [A]_{aq}} = \frac{HRL_{wc}T}{1 + HRL_{wc}T} \quad (25)$$

where R the ideal gas constant (in L atm mol⁻¹ K⁻¹), H the Henry's Law Constant (in M atm⁻¹), and L_{wc} is the dimensionless liquid water content of the cloud (typically 4.2×10^{-7}). L_{wc} is related to the condensed phase surface to gas volume ratio (cm²/cm³) A_c by the following equation:

$$A_c = \frac{6L_{wc}}{d} \quad (26)$$

where d is the diameter of droplets contained in tropospheric clouds (typically 50 μ m).⁵⁷

Mass accommodation can limit the rate of gas uptake. The accommodation time-scale τ_{accom} can be estimated from the mass accommodation coefficient α as

$$\tau_{accom} = \frac{1}{1/4\omega A_c \alpha} \quad (27)$$

The mass accommodation coefficients α have been determined in this work and their values at 298 K are respectively equal to 8.3×10^{-4} for 2-nitrophenol, 3.1×10^{-4} for 2-methylphenol, 7.3×10^{-4} for 2-methylphenol, and 1.2×10^{-3} for 4-methylphenol. From the values of α , the calculated accommodation time scale varies between 7 and 18 min. In regard to the tropospheric lifetimes of phenolic compounds in the gas phase (see Table 6), mass accommodation is indeed a fast process. Therefore, the uptake of these compounds by atmospheric droplets will not be limited by mass transport.

Assuming that equilibrium is effectively rapidly reached, eq 23 can be written as follows:

$$\tau_{A,multiphase} = \frac{1 + HRL_{wc}T}{(k_{OH,g}[OH]_g) + HRL_{wc}T(k_{OH,aq}[OH]_{aq})} \quad (28)$$

where $k_{OH,aq}$ is the rate constant of OH reaction with A in

TABLE 6: Rate Constants of OH Reaction with 2-Nitrophenol and Isomers of Cresols in Gaseous and Aqueous Phases and the Corresponding Henry's Law Constants at 298 K

compound	$k_{\text{OH,g}}^{298\text{K } a}$	$k_{\text{OH,aq}}^{298\text{K } d}$	$H^{298\text{K}}$ (M atm ⁻¹)	τ_{gas} (days)	$\tau_{\text{multiphase}}$ (days)
2-nitrophenol	$9.0 \times 10^{-13}{}^b$	$9.2 \times 10^9{}^e$	70 ^g	12.87	7.42
2-methylphenol	$4.9 \times 10^{-11}{}^c$	$1.1 \times 10^{10}{}^e$	433 ^h	0.24	0.22
3-methylphenol	$5.2 \times 10^{-11}{}^c$	—	791 ^h	0.22	0.19
4-methylphenol	$5.2 \times 10^{-11}{}^c$	$1.2 \times 10^{10}{}^f$	1101 ^h	0.23	0.18

^a In cm³ molecule⁻¹ s⁻¹. ^b Values reported by Atkinson et al.⁶⁰ ^c Semadeni et al.⁶¹ ^d In M⁻¹ s⁻¹. ^e Savel'eva et al.⁵⁸ ^f Feitelson and Hayon.⁵⁹ ^g US EPA.⁴⁹ ^h Feigenbrugel et al.⁶²

aqueous phase and [OH]_{aq} is the mean concentration of OH radicals in the tropospheric aqueous phase.

The rate constants of OH reaction with the studied compounds in both aqueous and gaseous phases have already been reported,^{58–61} and are shown in Table 6 together with the Henry's law constants given by US EPA for 2-nitrophenol,⁴⁹ and by Feigenbrugel et al.⁶² for isomers of cresols. By analogy with other methylphenols, the rate coefficient of OH reaction with 3-methylphenol was estimated to $1.2 \times 10^{10} \text{ M}^{-1} \text{ s}^{-1}$. These data have then been used to estimate the atmospheric lifetimes of these organic compounds under clear sky (τ_{gas}), and cloudy conditions ($\tau_{\text{multiphase}}$), by using typical concentrations of OH radicals in the gaseous and aqueous phases: [OH]_g = $1 \times 10^6 \text{ cm}^{-3}$ and [OH]_{aq} = $1 \times 10^{-13} \text{ M}$.⁶³ We assume here that the OH concentration in the gas phase is the same under clear sky and cloudy conditions although it is reduced as soon as clouds are formed, and the magnitude of the decrease strongly depends on the pH value of the droplets.⁶⁴

At 298 K, the calculated aqueous fractions are the following: 2-nitrophenol, 9.2×10^{-4} ; 2-methylphenol, 4.4×10^{-3} ; 3-methylphenol, 8.2×10^{-3} ; 4-methylphenol, 11.2×10^{-3} . At 298 K, the temperature at which most experimental rate constants were measured, the atmospheric lifetimes of methylphenols are slightly reduced in the clouds as shown in Table 6 whereas the impact of multiphase chemistry is more pronounced for 2-nitrophenol. However, the average temperature of tropospheric clouds is 283 K, and therefore, the calculated aqueous fraction of phenol rises when the temperature decreases from 298 to 283 K. Assuming that the rate constants of OH reactions with phenol or cresols in the gaseous and aqueous phases do not vary a lot between 283 and 298 K as it was already observed for many oxygenated volatile organic compounds, we can then estimate the multiphase lifetimes of these compounds at 283 K. These calculated lifetimes at 283 K (in units of days) are significantly lower than those at 298 K (in parentheses): 2-nitrophenol, 4.98 (7.42); 2-methylphenol, 0.17 (0.22); 3-methylphenol, 0.13 (0.19); 4-methylphenol, 0.11 (0.18). These results showed that aqueous phase reaction could have more impact on the global loss rate at 283 K than at 298 K for all studied compounds. Therefore gaseous and aqueous phase loss processes could really compete in tropospheric conditions. Mechanisms of OH oxidation in aqueous phase are therefore needed to identify the products that can be deposited to ground by wet deposition and consequently to better estimate the environmental impact of phenolic compounds.

Acknowledgment. Financial support for this work has been provided by the CNRS through the "Programme National de Chimie Atmosphérique" (PNCA). We are also grateful to the "Ministère de la Recherche et de l'Enseignement Supérieur", the "Région Nord/Pas de Calais", and the "Fonds Européen de Développement Economique des Régions" (FEDER) for funding of this work in the framework of the project "Qualité de l'air en milieux urbain et industriel: COV et particules" involved in

the "Contrat de Plan Etat Région" 2000-2006. We are grateful to anonymous reviewers for fruitful comments and discussion.

Supporting Information Available: Essential molecular parameters needed for the estimation of diffusion coefficients for studied species, diffusion coefficients calculated using the method of Brokaw, and corresponding mass accommodation coefficients. This material is available free of charge via the Internet at <http://pubs.acs.org>.

References and Notes

- (1) Allen, S. K.; Allen, C. W. *B. Environ. Contam. Tox.* **1997**, *59*, 702–707.
- (2) Leuenberger, C.; Czuczwa, J.; Tremp, J.; Giger, W. *Chemosphere* **1988**, *17*, 511–515.
- (3) Atkinson, R.; Aschmann, S. M.; Arey, J.; Carter, W. P. L. *Int. J. Chem. Kinet.* **1989**, *21*, 801–827.
- (4) Knispel, R.; Koch, R.; Siese, M.; Zetzsch, C. *Ber. Bunsen-Ges. Phys. Chem.* **1990**, *94*, 1375–1379.
- (5) Bjergbakke, E.; Sillesen, A.; Pagsberg, P. *J. Phys. Chem.* **1996**, *100*, 5729–5736.
- (6) Klotz, B.; Sørensen, S.; Barnes, I.; Becker, K. H.; Etzkorn, T.; Volkammer, R.; Platt, U.; Wirtz, K.; Martin-Reviejo, M. *J. Phys. Chem. A* **1998**, *102*, 10289–10299.
- (7) Smith, D. F.; Melver, C. D.; Kleindienst, T. E. *J. Atmos. Chem.* **1998**, *30*, 209–228.
- (8) Berndt, T.; Böge, O.; Herrmann, H. *Chem. Phys. Lett.* **1999**, *314*, 435–442.
- (9) Berndt, T.; Böge, O. *Phys. Chem. Chem. Phys.* **2001**, *3*, 4946–4959.
- (10) Volkammer, R.; Klotz, B.; Barnes, I.; Imamura, T.; Wirtz, K.; Washida, N.; Becker, K. H.; Platt, U. *Phys. Chem. Chem. Phys.* **2002**, *4*, 1598–1610.
- (11) Kawamura, K.; Kaplan, I. R. *Environ. Sci. Technol.* **1983**, *17*, 497–501.
- (12) Leuenberger, C.; Ligocki, M. P.; Pankow, J. F. *Environ. Sci. Technol.* **1985**, *19*, 1053–1058.
- (13) Herterich, R.; Herrmann, R. *Environ. Technol.* **1990**, *11*, 961–972.
- (14) Levsen, K.; Behnert, S.; Priess, B.; Svoboda, M.; Winkeler, H. D.; Zietlow, J. *Chemosphere* **1990**, *21*, 1037–1061.
- (15) Richartz, H.; Reischl, A.; Trautner, F.; Hutzinger, O. *Atmos. Environ.* **1990**, *24*, 3067–3071.
- (16) Grosjean, D. *Sci. Tot. Environ.* **1991**, *100*, 367–414.
- (17) Tremp, J.; Mattrel, P.; Fingler, S.; Giger, W. *Water Air Soil Poll.* **1993**, *68*, 113–123.
- (18) Lüttke, J.; Scheer, V.; Levsen, K.; Wünsch, G.; Cape, J. N.; Hargreaves, K. J.; Storenton-West, R. L.; Acker, K.; Wieprecht, W.; Jones, B. *Atmos. Environ.* **1997**, *31*, 2637–2648.
- (19) Lüttke, J.; Levsen, K. *Atmos. Environ.* **1997**, *31*, 2649–2655.
- (20) Belloli, R.; Barletta, B.; Bolzacchini, E.; Meinardi, S.; Orlandi, M.; Rindone, B. *J. Chromatogr. A* **1999**, *846*, 277–281.
- (21) Lüttke, J.; Levsen, K.; Acker, K.; Wieprecht, W.; Möller, D. *Int. J. Environ. Anal. Chem.* **1999**, *74*, 69–89.
- (22) Schmidt-Bäumler, K.; Heberer, T.; Stan, H. J. *Acta Hydrochim. Hydrobiol.* **1999**, *27*, 143–149.
- (23) Morville, S.; Scheyer, A.; Mirabel, P.; Millet, M. A. *Changing Atmosphere. 8th European Symposium on the Physico-Chemical Behavior of Atmospheric Pollutants*; Torino, Italy, 2001.
- (24) Davidovits, P.; Hu, J. H.; Worsnop, D. R.; Zahniser, M. S.; Kolb, C. E. *Faraday Discuss.* **1995**, *100*, 65–81.
- (25) Hanson, D. R.; Burkholder, J. B.; Howard, C. J.; Ravishankara, A. R. *J. Phys. Chem.* **1992**, *96*, 4979–4985.
- (26) Jayne, J. T.; Duan, S. X.; Davidovits, P.; Worsnop, D. R.; Zahniser, M. S.; Kolb, C. E. *J. Phys. Chem.* **1991**, *95*, 6329–6336.

- (27) Danckwerts, P. V. *Gas-Liquid Reactions*; McGraw-Hill: New York, 1970.
- (28) US EPA. Method TO-8 "Method for the determination of phenol and methylphenols (cresols) in ambient air using high performance liquid chromatography", <http://www.epa.gov/ttn/amtic/files/ambient/airtox/to-8.pdf>
- (29) Müller, B.; Heal, M. R. *J. Phys. Chem. A* **2002**, *106*, 5120–5127.
- (30) Utter, R. G.; Burkholder, J. B.; Howard, C. J.; Ravishankara, A. R. *J. Phys. Chem.* **1992**, *96*, 4973–4979.
- (31) Rudich, Y.; Talukdar, R. K.; Fox, R. W.; Ravishankara, A. R. *J. Geophys. Res.* **1996**, *101*, 21023–21031.
- (32) Rudich, Y.; Talukdar, R. K.; Imamura, T.; Fox, R. W.; Ravishankara, A. R. *Chem. Phys. Lett.* **1996**, *261*, 467–473.
- (33) Imamura, T.; Rudich, Y.; Talukdar, R. K.; Fox, R. W.; Ravishankara, A. R. *J. Phys. Chem. A* **1997**, *101*, 2316–2322.
- (34) Schweitzer, F.; Mirabel, P.; George, C. *J. Phys. Chem. A* **1998**, *102*, 3942–3952.
- (35) Fickert, S.; Helleis, F.; Adams, J. W.; Moortgat, G. K.; Crowley, J. N. *J. Phys. Chem. A* **1998**, *102*, 10689–10696.
- (36) Fickert, S.; Adams, J. W.; Crowley, J. N. *J. Geophys. Res.* **1999**, *104*, 23719–23727.
- (37) Müller, B.; Heal, M. R. *Phys. Chem. Chem. Phys.* **2002**, *4*, 3365–3369.
- (38) Howard, C. J. *J. Phys. Chem.* **1979**, *83*, 3–9.
- (39) *CRC Handbook of Chemistry and Physics*, 82th ed.; CRC Press: Boca Raton, FL, 2001.
- (40) Murphy, D. M.; Fahey, D. W. *Anal. Chem.* **1987**, *59*, 2753–2759.
- (41) Reid, R. C.; Prausnitz, J. M.; Poling, B. E. *The Properties of Gases and Liquids*, 4th ed.; McGraw-Hill: New York, 1987.
- (42) Wilke, C. R.; Lee, C. Y. *Ind. Eng. Chem.* **1955**, *47*, 1253–1257.
- (43) (a) Fuller, E. N.; Giddings, J. C. *J. Gas Chromatogr.* **1965**, *3*, 222–227. (b) Fuller, E. N.; Schettler, P. D.; Giddings, J. C. *Ind. Eng. Chem.* **1966**, *58*, 19–27. (c) Fuller, E. N.; Ensley, K.; Giddings, J. C. *J. Phys. Chem.* **1969**, *73*, 3679–3685.
- (44) Schweitzer, F.; Magi, L.; Mirabel, P.; George, C. *J. Phys. Chem. A* **1998**, *102*, 593–600.
- (45) Katrib, Y.; Deiber, G.; Mirabel, P.; Le Calvé, S.; George, C.; Mellouki, A.; Le Bras, G. *J. Atmos. Chem.* **2003**, *43*, 151–174.
- (46) Guanghua, L.; Jie, T.; Xing, Y.; Yuanhui, Z. *Chem. J. Internet* **2001**, *3*(4): 15–18.
- (47) Brokaw, R. S. *Ind. Eng. Chem. Process Design Dev.* **1969**, *8*, 240.
- (48) Schwartz, S. E.; Freiberg, J. E. *Atmos. Environ.* **1981**, *15*, 1129–1144.
- (49) US EPA. *Air and stream stripping of toxic pollutants. Technol. Rep. EPA-68-03-002*. Industrial Environmental Research Laboratory, Cincinnati, OH, 1982.
- (50) Jayne, J. T.; Duan, S. X.; Davidovits, P.; Worsnop, D. R.; Zahniser, M. S.; Kolb, C. E. *J. Phys. Chem.* **1992**, *96*, 5452–5460.
- (51) Worsnop, D. R.; Zahniser, M. S.; Kolb, C. E.; Gardner, J. A.; Watson, L. R.; Van Doren, J. M.; Jayne, J. T.; Davidovits, P. *J. Phys. Chem.* **1989**, *93*, 1159–1172.
- (52) Nathanson, G. M.; Davidovits, P.; Worsnop, D. R.; Kolb, C. E. *J. Phys. Chem.* **1996**, *100*, 13007–13020.
- (53) Raja, S.; Valsaraj, K. T. *Environ. Sci. Technol.* **2004**, *38*, 763–768.
- (54) Atkinson, R. *Atmos. Environ.* **2000**, *34*, 2063–2101.
- (55) Ervens, B.; Gligorovski, S.; Herrmann, H. *Phys. Chem. Chem. Phys.* **2003**, *5*, 1811–1824.
- (56) Monod, A.; Poulain, L.; Grubert, S.; Voisin, D.; Wortham, H. *Atmos. Environ.*, submitted for publication.
- (57) Kolb, C. E.; Worsnop, D. R.; Zahniser, M. S.; Davidovits, P.; Hanson, D. R.; Ravishankara, A. R.; Keyser, L. F.; Leu, M. T.; Williams, L. R.; Molina, M. J.; Tolbert, M. A. *Laboratory Studies of Atmospheric Heterogeneous Chemistry. In Advanced Series in Physical Chemistry*; Barker, J. R., Ed.; World Scientific: Singapore, 1995; Vol. 3, p 771.
- (58) Savel'eva, O. S.; Shevchuk, L. G.; Vysotskaya, N. A. *J. Org. Chem. USSR* **1972**, *8*, 283–286.
- (59) Feitelson, J.; Hayon, E. *J. Phys. Chem.* **1973**, *73*, 10–15.
- (60) Atkinson, R.; Aschmann, S. M.; Arey, J. *Environ. Sci. Technol.* **1992**, *26*, 1397–1403.
- (61) Semadeni, M.; Stocker, D. W.; Kerr, J. A. *Int. J. Chem. Kinet.* **1995**, *27*, 287–304.
- (62) Feigenbrugel, V.; Le Calvé, S.; Mirabel, P.; Louis, F. *Atmos. Environ.* **2004**, *38*, 5577–5588.
- (63) Ervens, B.; George, C.; Williams, J. E.; Buxton, G. V.; Salmon, G. A.; Bydder, M.; Wilkinson, F.; Dentener, F.; Mirabel, P.; Herrmann, H. *CAPRAM 2.4 J. Geophys. Res.* **2003**, *108*(D14), 4426.
- (64) Monod, A.; Carlier, P. *Atmos. Environ.* **1999**, *33*, 4431–4446.